COBEM 2023 27TH INTERNATIONAL CONGRESS OF MECHANICAL ENGINEERING

ABCM Brazilian Society of Mechanical Sciences and Engineering
27th ABCM International Congress of Mechanical Engineering
December 04-08, 2023, Florianópolis-SC, Brazil

COB-2023-2432
HIGH-SPEED AND INFRARED FLOW BOILING VISUALIZATION IN MICROCHANNELS WITH MODIFIED SURFACES

Mariana Perez
Pedro Pontes
Ana Moita
IN+, Centro de Estudos em Inovação, Tecnologia e Políticas de Desenvolvimento, Instituto Superior Técnico, Universidade de Lisboa, Lisboa, Portugal
mariana.perez@tecnico.ulisboa.pt
pedro.daniel.pontes@tecnico.ulisboa.pt
anamoita@tecnico.ulisboa.pt

Abstract. *The present research aims to study the effect of microchannel cooling using two phase flow. With the aim of enhancing heat transfer and flow stability, surface modifications were investigated. Two stainless steel surfaces were tested, a smooth surface and one with two 100 um cavities 200 um apart. The setup included a single microchannel, manufactured in PDMS and placed on the heated surfaces. Results were obtained using two different techniques, infrared thermography and high speed images while pressure drop on the channel was also measured. Two different power values were supplied and two different flow rates were considered. Pressure drop results were inconclusive of the effect of surface indentations. The images taken allowed visualization of nucleation sites, and confirmed that none were found near the cavities. Nevertheless, the analysis proposed was able to identify where nucleation sites were formed. Slug flow interfacial heat transfer could be observed and accurately described in the thermal and heat transfer maps.*

Keywords:Microchannels, Two-phase flows, Interfacial heat transfer

1. INTRODUCTION

There has been a wide interest in designing better and more efficient cooling devices, which is an essential need of more power intensive technologies being created. In the field of concentrator photovoltaics, the challenge has been addressing the higher cost by decreasing conversion losses, which can be done with efficient thermal management. In this sense many have suggested microchannel liquid based heat sinks as a solution, as they show low thermal resistances in comparison with other technologies (Royne *et al.* (2005)). Also here studies have been focusing in alternative geometries, fluids or two phase flows as a way to further improve their performance (Gilmore *et al.* (2018)).

Valeh-e Sheyda *et al.* (2013) did a comparative study of two phase flow and single phase cooling using water as the working fluid, specifically for slug flow. Results show a much higher cell performance for two-phase flow with higher rates of heat transfer. The potential of two phase flows lies in the additional latent heat removed during evaporation. But highly unstable flow condition and pressure losses are inevitable. So, in order to understand the boiling phenomena inside the microchannels, visualization techniques may present advantages and improve the analysis. Mohammadi and Sharp (2013) presented a review on the different techniques used for bubble dynamics analysis in microchannels, some of which are: high speed photography, fluorescent microscopy and magnetic resonance with High-speed imaging being the most used technique. In regards to thermal measurements, Liu and Pan (2016) also explored the use of infrared thermography, which presented results showing that this technique can help identify temperature distribution in the two-phase region. The majority of the existing studies on microchannel two-phase flow are analysed with only high-speed imagery while IR techniques can complement this results. The combination of both techniques can provide valuable insight to the heat transfer mechanisms present inside the channels.

Despite having influence on the heat extracted, the phase of the fluid is not the only parameter that can change in order to enhance heat transfer. Different studies on application of surface roughness, cavities and fins have been a focus of research over the years. Tullius *et al.* (2011) presents a review of microchannel cooling with emphasis on different surface modifications for both single and two-phase flow concluding that these modifications contribute to an improved cooling performance.

In this work the aim is to infer the influence of surface cavities in improving heat transfer in microchannels with two-phase and flow stability by controlling where nucleation sites appear. To do this, a transparent single channel configuration is being used with a combination of high-speed imaging and infrared thermography with high temporal resolution. A smooth surface will be compared against a surface with two cavities under different working conditions.

2. METODOLOGY

2.1 Experimental set-up

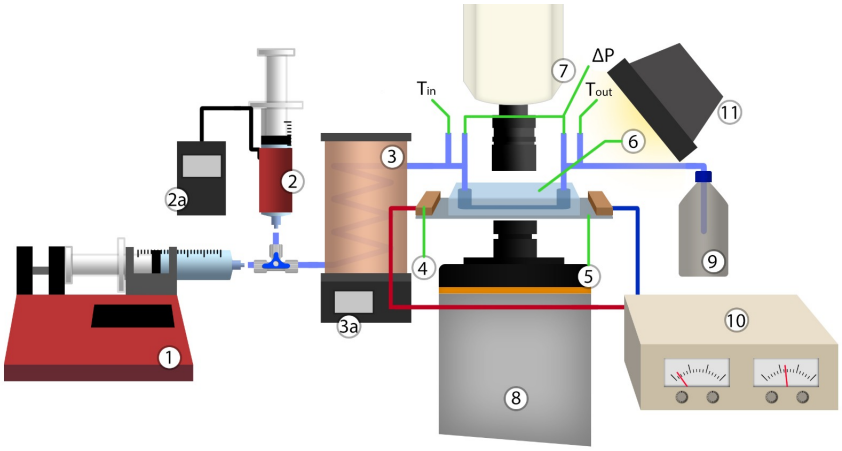

Figure 1. Experimental installation scheme: 1) Syringe Pump; 2) Heated syringe for Degasification with Temperature Controller (2a.); 3) Thermal Bath with Temperature Controller (3a.); 4) Electric contacts; 5) Stainless steel foil (10μm thick); 6) PDMS microchannel prototype; 7) High-speed camera; 8) Thermographic camera; 9) Output HFE-7100 Container; 10) DC Power Supply; 11) Light Source

The experimental setup is schematicaly depticted in Figure 1. First, the PDMS microchannel is placed on top of a stainless steel sheet (Figure 1: 6,5), pressure sealed by an acrylic plate. To simulate the heating of the solar cells, the stainless steel sheet (Figure 1: 5) is connected to electric contacts (Figure 1: 4) on both ends of the sheet. These contacts are connected to a DC Power Supply (Figure 1: 10). This way, the sheet is heating by Joule effect, and the heating is controlled by regulating the provided current. Placed between the stainless steel foil and the channel is a thermocouple type K that registers the foil temperature.

The used fluid, 3M NOVEC HFE7100, begins its process in the degasification station (Figure 1: 2 and 2a) where the fluid is heated up to its boiling point inside a syringe with a heating pad. This heating pad has a temperature control device which is set at 60 °C. After degasification and cooling, the fluid goes into the syringe that is placed on the syringe pump (Figure 1: 1). This pump allows the control of the volumetric fluid flow that will enter the channel. The fluid then passes through a thermal bath of oil (Figure 1: 3 and 3a), allowing the fluid to be heated before entering the channel. This thermal bath is also set to 60 °C so that the fluid may enter the channel with temperature conditions close to saturation. When leaving the thermal bath, the fluid enters the test section where it goes through the boiling process and afterwards goes into a reservoir (Figure 1: 9) at atmospheric pressure.

During the experiments, data is being collected in order to better understand the changes inside the channel. Visual characterization of the channel is done using a High-speed camera (Figure 1: 7) that is place directly above the channel, perpendicularly, and allows to observe bubbles formation. The light source in Figure 1: 11 is required for the High speed camera in order to observe the process inside the channel. Also, directly below the sheet is a Thermographic camera Figure 1: 8) that detects temperature change on the stainless-steel sheet. Temperature at the entrance and exit of the channel is registered using two type K thermocouples, equal to the one used to measure the foil temperature. Additionally, pressure difference between inlet and outlet is measured using a differential pressure sensor.

2.2 Test conditions

The chosen working fluid for this project was HFE-7100. The inlet temperature range set to be 45-55C maximum. For temperatures above this, the bubbles seen are mainly slugs coming from the thermal bath, and below, boiling is difficult to achieve. There are some fluid characteristics that make HFE 7100 an interesting fluid to work with: its boiling point at 61 °C (3M (2023)), which makes it easier to combine with other materials when working with boiling conditions, namely acrylic. This is a dielectric fluid, which means it prevents flow of electric current. Furthermore it requires less energy to reach the desired conditions to perform tests.

For the same conditions as the ones tested in this research, Gonçalves (2022) tested three different heat fluxes and presents the temperature values of the sheet during the tests, for each heat flux imposed. The minimum sheet temperature should be set to a temperature close to the boiling temperature of the working fluid - 61 °C or a temperature that allows bubble formation during the tests. This minimum sheet temperature was obtained for a current of 3.6 A, corresponding to a heat flux of 1346 W/m^2. The maximum temperature of the sheet has in consideration the surrounding materials,

namely the top acrylic plate which should not be exposed to temperatures above 80 °C which is reached providing a current of 3.97 A to the stainless-steel sheet (corresponding to 1637 W/m^2). Table 1 compiles the current values used for the stainless-steel sheet with no cavities and corresponding heat fluxes as well as equivalent current used for the sheet with 2 cavities in order to maintain a constant heat flux throughout the tests. Despite only testing two heat fluxes, it is still possible to draw conclusions of its influence on the flow inside the microchannel. The heat fluxes evaluated are comprehended in between the two lowest heat fluxes tested by Gonçalves (2022) as well as intermediate volumetric flow rates, meaning that results taken from this research complement the ones obtained previously.

Table 1. Imposed current and respective heat flux for each Stainless-steel sheet used.

I[A] (No cavities)	q [W]	q"[W/m2]	I[A] (2 Cavities)
3,60	1.46	1346	3,41
3,97	1.77	1637	3,76

The volumetric flow rate was defined based on the Reynolds number associated with each channel and can be found in Tab. 2. All flow rates evaluated in this research correspond to Reynolds numbers lower than 2300, which means it is focused on the laminar regime.

Table 2. Volumetric flow rates used and corresponding Reynolds number

Reynolds Number	u_m [m/s]	Q [ml/min]
70	0,019	1,114
120	0,032	1,910

2.2.1 Microchannel production and geometric details

The microchannels used were produced in PDMS, Polydimethylsiloxane during the preparation and set-up of the experimental apparatus. This material has properties like being transparent and self-sealing that are important advantages for the research being done, namely, avoiding the need for sealing the microchannel with an extra material, and allowing a clear vision of the channel, with the high speed camera and at naked eye, for leakages.

The production process of the microchannels followed the technique described by Gonçalves (2022). Initially, the 3D printed molds were involved in aluminium tape forming a rectangular shaped parallelepipe with no top, shown in Figure 2. It is important to ensure that the adhesive part of the tape is not on the inside, to prevent it from gluing to the PDMS when dry. The PDMS mixture used consists of Sylgard 184 elastometer and a curing agent with ratio of 10:1. The curing time for the mixture to be finished depends on the mass ratio used and the temperature at which it is left to dry, which in this case is 48h (Miranda *et al.* (2021)). When dry, it can be removed from the mold carefully. It is important to verify if there is any air bubble present, specially if it is located on the channel area. The holes for fluid inlet and outlet are the last procedure and it is done manually, according to the mold geometry. The channel used in this research has a rectangular geometry of 1:1mm.

The stainless-steel foils used have a similar rectangular geometry and a thickness of 2 mm. With reference to the sheet with 2 cavities, the cavities' diameter is 100 μm and distance between cavities is 200 μm.

2.3 Image post processing

The high speed videos were converted into image batches and processed using a MATLAB routine, which includes a background removal and contrast adjustment.

The videos from the IR camera were extracted with raw data from the software, and a custom made calibration was applied to transform the data into degrees Celsius. After this a median filter was applied to the values to eliminate noise in the data. Finally the surface local heat flux (q'') was calculated using an energy balance on the stainless steel foil surface, shown in eq. 1.

$$q'' = q_i'' + k_{sst}\lambda_{sst}(\frac{D^2T}{Dx^2} + \frac{D^2T}{Dy^2}) - cp_{sst}\rho_{sst}\lambda_{sst}\frac{DT}{Dt} \tag{1}$$

Figure 2. Microchannel mold with aluminium tape for PDMS microchannel production.

Here, q_i'' represents a source term and its value is the supplied heat flux for the specific case, k_{sst} is the stainless steel thermal conduction, λ_{sst} is the thickness of the stainless steel foil, cp_{sst} is its specific heat and ρ_{sst} the density.

3. RESULTS

3.1 Pressure drop

Pressure drop results in the microchannel can be seen in Figure 3. Especially when looking at the pressure drop, the noticeable error bars with the higher heat flux show the high variability between measurements. This behaviour is explained by the constant clogging of the channel with vapour slugs, back flow and unpredictable activation and deactivation of nucleation sites. With this considered there was no noticeable impact of the cavities in the pressure drop, showing very similar results.

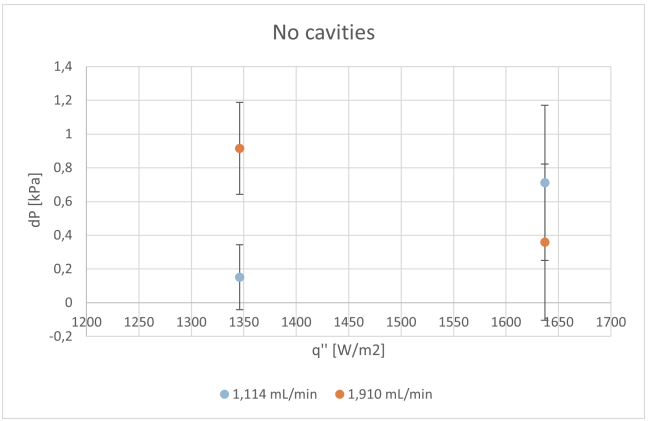

a)

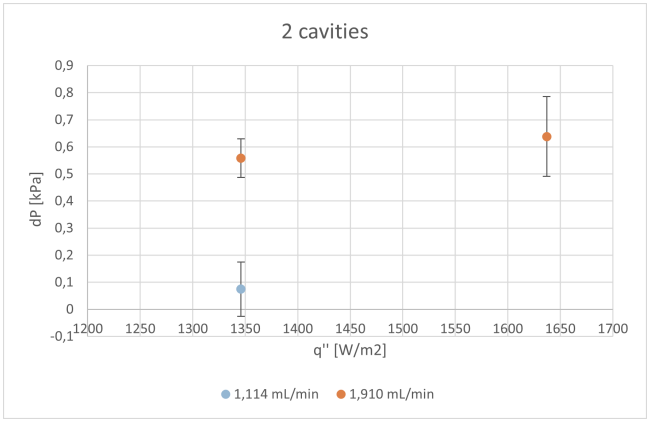

b)

Figure 3. Pressure drop between the inlet and outlet: a) Sheet with no cavities, b) Sheet with two cavities.

3.2 High Speed vs Infrared Thermography Analysis

On a first analysis the nucleation sites were analysed and compared on the 2 cavity foil. In Figure 4 an example of the 3 different types of images can be seen: the high-speed image, a temperature map and a local heat flux map. Although the cavities are inside the channel, they weren't activated as nucleation sites with the heat flux provided. Instead it is possible to see 3 different nucleation sites in the figure. While in the high speed image is less visible, and can only be seen by detecting the origin of smaller vapour bubbles, in both the thermal and heat flux images these sites are visible. In the temperature image the nucleation sites have a lower temperature of approximately 1.5 °C around them and in the heat flux image it is possible to see a higher heat flux of around 4000 W/m^2 in the sites. The example presented shows increased heat transfer is present in the region where evaporation occurs thus decreasing the local surface temperature.

Although the objective of adding cavities was to create possible nucleation sites, these were never activated, and usually the activated sites were on the contact line between the PDMS and stainless steel. This is likely due to the

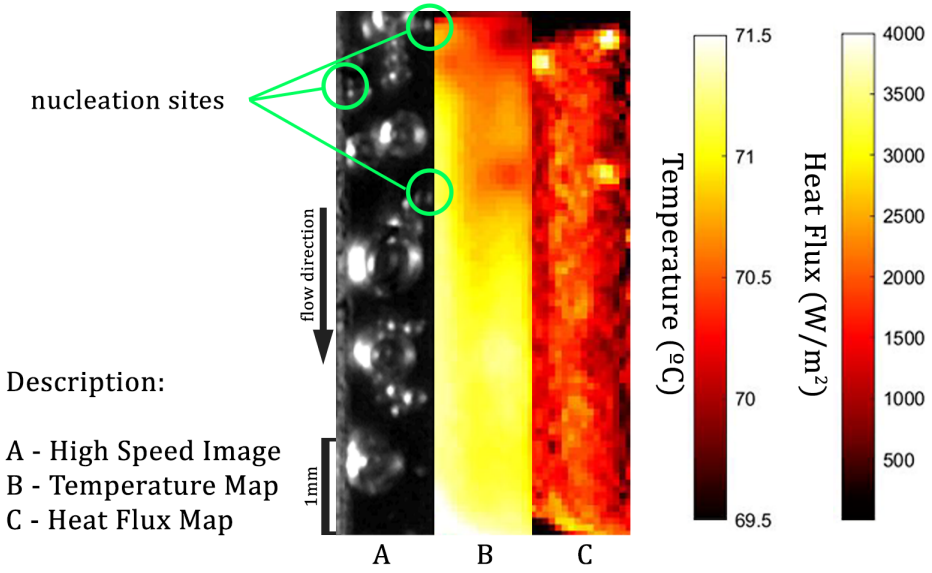

Figure 4. Images captured with the high-speed camera and respective temperature and heat flux obtained with the images taken with the IR camera showing active nucleation sites. (Stainless-steel sheet with 2 cavities; Heat flux: 1637 W/m^2; Volumetric flow rate: 1.910 ml/min)

insulation provided by the PDMS which increases temperature in the heated surface near the wall.

Even though the placement of nucleation sites would change during the tests, it was possible to observe interfacial heat transfer phenomena during vapour slug development. An example of this can be seen in Figure 5.

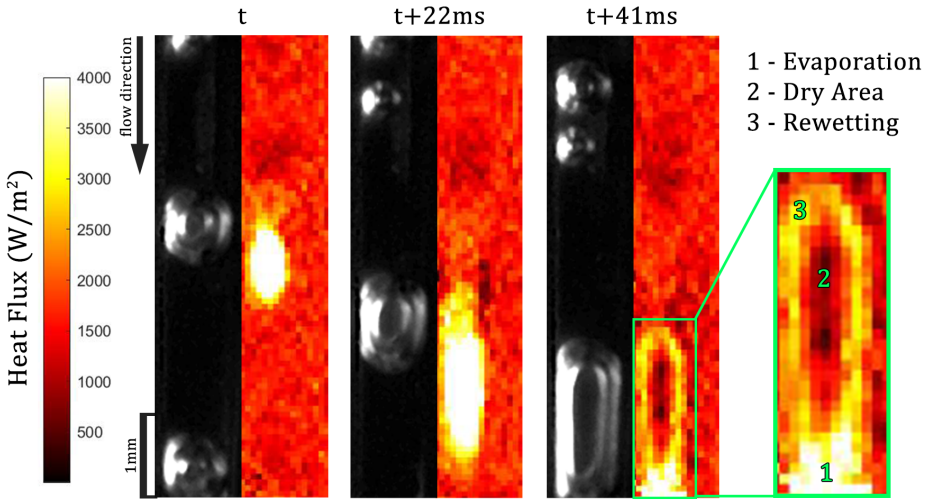

Figure 5. Images captured with the high-speed camera and respective temperature and heat flux obtained with the images taken with the IR camera showing growth and movement of a slug along the microchannel. (Stainless-steel sheet with 2 cavities; Heat flux: 1637 W/m^2; Volumetric flow rate: 1.910 ml/min)

In this Figure a bubble that traverses the channel grows through surface evaporation into a slug. Initially, when its size is smaller, bellow it it's possible to observe an area of increased heat flux. Notice that here the full area has phase change occurring on a thin liquid layer bellow. The bubble then enlongates and so does the high heat flux patch. In the final frame (t+41ms), it is possible to see the effect of a dry area, as the slug grows and the vapour is in direct contact with the heated surface. In this area the vapour is insulating the surface from the convection heat transfer. Around the slug, one can observe a higher heat flux of around 3500 W/m^2. Here, near the 3 phase contact line evaporation keeps occurring while in the back of the slug the rewetting phenomenon can also be seen. This can be better observed when accompanied by looking at an example in Figure 6.

In this figure, we have a view from the side, using high-speed imaging, of a bubble developing into a slug. In the earlier stages a thin liquid film is visible in between the vapour mass and the heated surfaces, while in later stages the slug

comes into full contact with the surface. Note that this image is taken from a different ongoing work to illustrate the case presented.

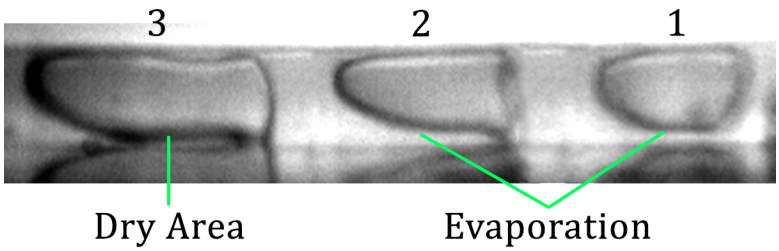

Figure 6. Slug development example

4. CONCLUSIONS

In this work, the influence of surface indentations in two phase microchannel flow was studied. The instability of the flow made it impossible to conclude if the surface modification had any impact on the pressure drop.

Through analyzing high-speed images synchronized with infrared images, it was possible to confirm that the presence cavities had indeed no effect on the performance of the system. Furthermore, it was possible to detect where nucleation sites were in the thermal maps but none was detected near the indentations. In future works higher number of indentations should be looked into to infer if this type of modification can have impact on the heat sink performance.

The methodology used proved to be an effective analysis tool to look into interfacial heat transfer phenomena providing temperature and heat flux maps that can able us to better understand them.

5. REFERENCES

3M, 2023. *3M Novec™ Engineered Fluid HFE-7100 for Heat Transfer*.

Gilmore, N., Timchenko, V. and Menictas, C., 2018. "Microchannel cooling of concentrator photovoltaics: A review". *Renewable and Sustainable Energy Reviews*, Vol. 90, pp. 1041–1059.

Gonçalves, I.A.A., 2022. *Escoamento Multifásico em Microcanais: Estudo para aplicação a um sistema de refrigeração de painéis fotovoltaicos de alta concentração*. Master's thesis, Instituto Superior Técnico.

Liu, T.L. and Pan, C., 2016. "Infrared thermography measurement of two-phase boiling flow heat transfer in a microchannel". *Applied thermal engineering*, Vol. 94, pp. 568–578.

Miranda, I., Souza, A., Sousa, P., Ribeiro, J., Castanheira, E.M., Lima, R. and Minas, G., 2021. "Properties and applications of pdms for biomedical engineering: A review". *Journal of functional biomaterials*, Vol. 13, No. 1, p. 2.

Mohammadi, M. and Sharp, K.V., 2013. "Experimental techniques for bubble dynamics analysis in microchannels: a review". *Journal of fluids engineering*, Vol. 135, No. 2, p. 021202.

Royne, A., Dey, C.J. and Mills, D.R., 2005. "Cooling of photovoltaic cells under concentrated illumination: a critical review". *Solar energy materials and solar cells*, Vol. 86, No. 4, pp. 451–483.

Tullius, J.F., Vajtai, R. and Bayazitoglu, Y., 2011. "A review of cooling in microchannels". *Heat Transfer Engineering*, Vol. 32, No. 7-8, pp. 527–541.

Valeh-e Sheyda, P., Rahimi, M., Karimi, E. and Asadi, M., 2013. "Application of two-phase flow for cooling of hybrid microchannel pv cells: a comparative study". *Energy Conversion and Management*, Vol. 69, pp. 122–130.

6. RESPONSIBILITY NOTICE

The authors are solely responsible for the printed material included in this paper.